Dalton Transactions

An international journal of inorganic chemistry

www.rsc.org/dalton

Number 28 | 28 July 2008 | Pages 3621–3760

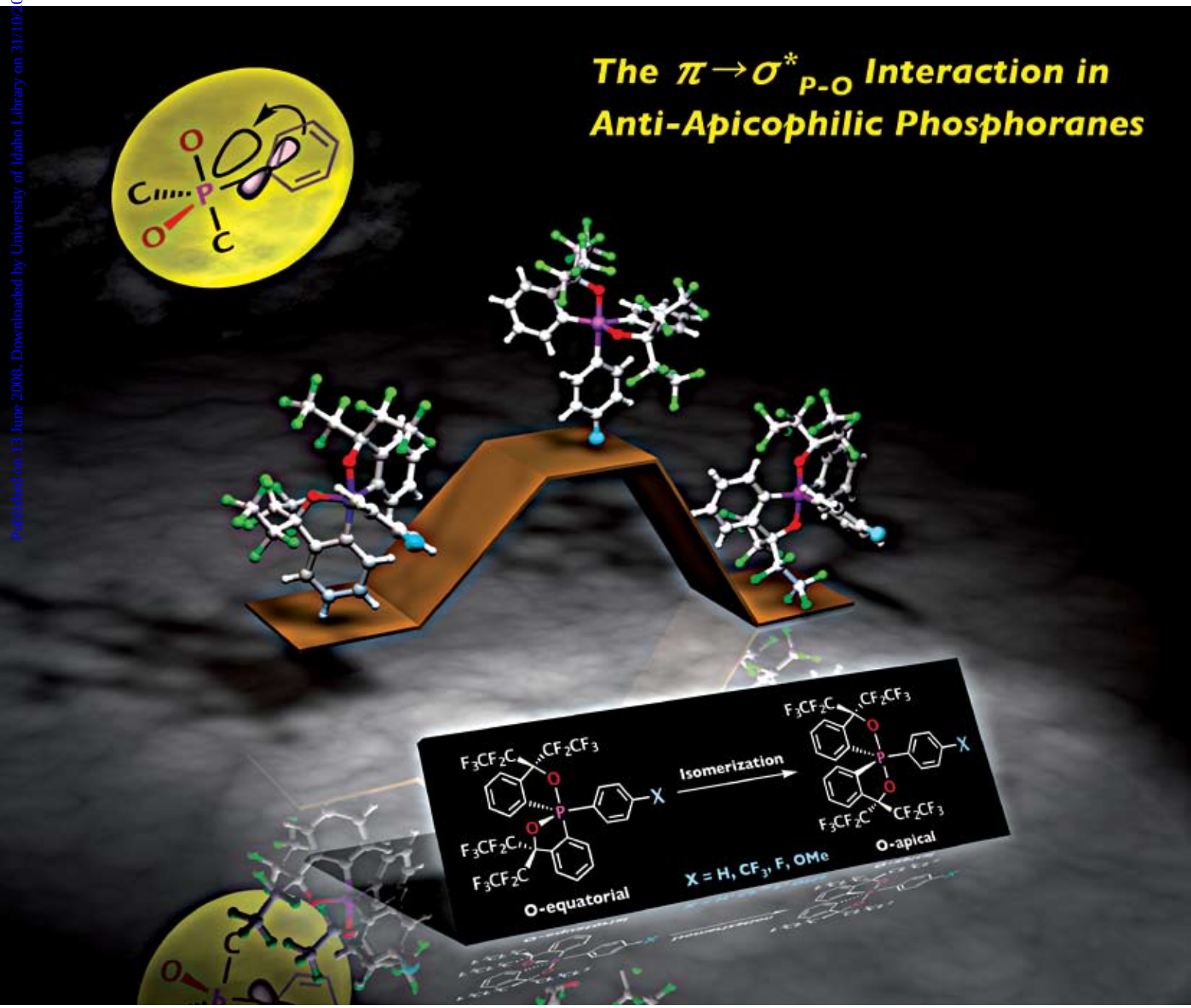

ISSN 1477-9226

PAPER
Yamamoto *et al.*
Synthesis, structure and isomerization of arylphosphoranes with anti-apicophilic bonding modes using a novel bidentate ligand with two C_2F_5 groups

HOT PAPER
Linti and Seifert
A decagallane(6) cluster $Ga_{10}[Si(CMe_3)_3]_6$ with an unprecedented structure

RSC Publishing

Synthesis, structure and isomerization of arylphosphoranes with anti-apicophilic bonding modes using a novel bidentate ligand with two C_2F_5 groups†

Xin-Dong Jiang, Shiro Matsukawa and Yohsuke Yamamoto*

Received 20th February 2008, Accepted 12th May 2008
First published as an Advance Article on the web 13th June 2008
DOI: 10.1039/b802947d

A series of anti-apicophilic pentacoordinate phosphoranes (with one chelating substituent in an O-equatorial, C-apical bonding mode at pentacoordinated phosphorus atom) bearing a *para*-substituted aryl group (–C_6H_4(*p*-X); X = H, CF_3, F, OMe) or a mesityl (2,4,6-trimethylphenyl) group were isolated using a novel bulky bidentate ligand with two C_2F_5 groups. These phosphoranes were stable to isomerization at room temperature, and quantitatively converted into the corresponding more stable isomers (O-apical) at elevated temperatures in solution. On the basis of a kinetic study, the free energy of activation ($\Delta G^{\ddagger}$) of the stereomutation of the O-equatorial mesitylphosphorane to its O-apical isomer was higher than that of the CF_3 derivative by 2.6 kcal mol^{-1}, giving rise to a further example of the steric effect of the C_2F_5 group to freeze the isomerization of the pentacoordinate phosphorus compounds. Kinetic measurements of the isomerization of the O-equatorial *ortho*-unsubstituted derivatives (–C_6H_4(*p*-X)) to the corresponding O-apical isomers suggested that the O-equatorial isomers were stabilized by the $\pi \rightarrow \sigma^*_{P\text{-}O}$ interaction in the ground state.

Introduction

Hypervalent[1] 10-P-5[2] phosphorus compounds (phosphoranes) are regarded as intermediates (or transition states) in the formation or hydrolysis of biologically relevant phosphorus compounds[3] such as DNA or RNA. Furthermore, they also play important roles as intermediates in the Wittig reaction.[4] Phosphorane chemistry is crucially important to understand the mechanisms of the above-described reactions, thus, a number of studies on phosphoranes have been carried out to establish many important properties.[5] However, phosphorane chemistry is still complicated due to their kinetic and thermodynamic properties. Phosphoranes generally prefer a trigonal-bipyramid (TBP) structure which has two distinct bonds, *i.e.*, an apical bond and equatorial bond. The apical bond is described as a three-center–four-electron (hypervalent) bond whereas the equatorial bond is described as an sp^2 bond. The former is more polar than the latter, and the apical site is sterically more congested than the equatorial site,[6] therefore, the electronegative and sterically less bulky groups prefer the apical site. The relative preference of substituents occupying the apical site is specifically known as apicophilicity.[7,8] From a kinetic standpoint, on the other hand, a pentacoordinate molecule causes rapid stereomutations, giving rise to an exchange between the apical and equatorial ligand, therefore, such a molecule generally exists as an equilibrium mixture containing several (up to 20) stereoisomers in the solution state. This nondissociative intramolecular site exchange of substituents is usually advocated by the Berry pseudorotation (BPR).[9,10] The barrier to the BPR is very low (calculated to be about 2–3 kcal mol^{-1} for PH_5)[11] without any steric restrictions.

Using the rigid bidentate ligand called the Martin ligand (**A**),[12] our group succeeded in synthesizing the anti-apicophilic phosphoranes (with one chelating substituent in an O-equatorial, C-apical bonding mode at pentacoordinated phosphorus atom) having an alkyl monodentate ligand (O-equatorial **1**) (Fig. 1).[13] Unlike the case of other anti-apicophilic phosphoranes,[14] these O-equatorial phosphoranes are kinetically stabilized products, and can still be converted into the corresponding more stable stereoisomers (O-apical **2**). Although the Martin ligand is capable of stabilizing various types of hypervalent compounds both thermodynamically and kinetically, isolation of the O-equatorial phosphoranes bearing a small or electronegative monodentate ligand has still been troublesome because such compounds are isomerized too fast to be isolated. For example, the O-equatorial **1a** (R = Me) could not be isolated in the pure form because the

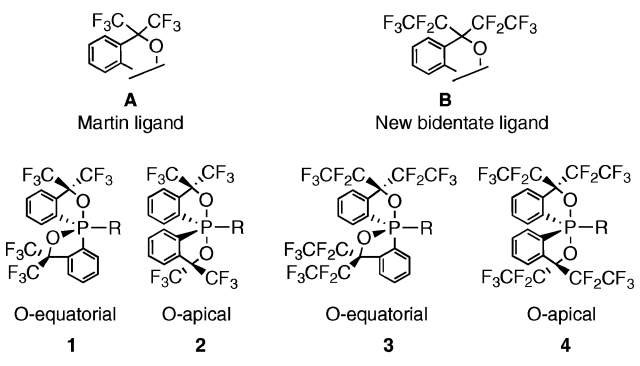

Fig. 1 Phosphoranes bearing bidentate ligands for freezing BPR.

Department of Chemistry, Graduate School of Science, Hiroshima University, 1-3-1 Kagamiyama, Higashi-Hiroshima, 739-8526, Japan. E-mail: yyama@sci.hiroshima-u.ac.jp; Fax: +81-82-424-0723

† CCDC reference numbers 672351 (**12a**), 672352 (**12b**), 672353 (**12c**), 672354 (**12d**), 672355 (**12e**), 672356 (**13d**) and 672357 (**13e**). For crystallographic data in CIF or other electronic format see DOI: 10.1039/b802947d

irreversible isomerization of **1a** to **2a** was relatively fast. Thus, we developed a bulky bidentate ligand with two C_2F_5 groups (**B**) in place of the CF_3 groups of the Martin ligand.[15] This allowed us to isolate the O-equatorial methylphosphorane **3a** in the pure form, and the free energy of activation ($\Delta G^{\ddagger}_{333}$) of the isomerization of **3a** to **4a** was found to be greater than that of **1a** to **2a** by 3.6 kcal mol^{-1}. Furthermore, ligand **B** was also effective for freezing the isomerization of the "anti-apicophilic" 10-As-5 arsoranes (O-equatorial, C-apical) to the more stable stereoisomers (O-apical, C-equatorial).[16]

As a more electronegative monodentate ligand than the alkyl group, we chose aryl groups as the next targets. Although several attempts were made to isolate the O-equatorial arylphosphoranes **5** using the Martin ligand (**A**), it was found that these phosphoranes, except for the TIP (2,4,6-triisopropylphenyl) derivative **5c**, rapidly isomerized to the O-apical counterparts (Scheme 1).[17] For example, the isomerization of the phenyl derivative (**5a** to **6a**) was completed within 30 min at r.t., which was in contrast to the O-equatorial alkyl derivatives (**1**). We assumed that the stereomutation of the O-equatorial to O-apical isomer passes through a high-energy intermediate (**Int-1**) which bears the monodentate ligand (R) at the apical site, therefore, the more apicophilic R could accelerate the isomerization (Scheme 2). Thus, the rapid isomerization was mainly due to the much higher apicophilicity of the aryl group than the alkyl group.[7b,c,i,j] This required employing a very bulky TIP group to isolate the O-equatorial isomer.

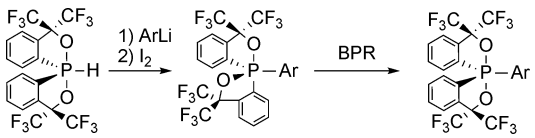

Ar	Ratio of O-equatorial **5**/O-apical **6**			
	O-equatorial	O-apical	directly after	after 30 min.
Ph	**5a**	**6a**	27:73	<1:>99
Mes	**5b**	**6b**	>99:<1	62:38
TIP	**5c**	**6c**	>99:<1	>99:<1

Mes = 2,4,6-trimethylphenyl, TIP = 2,4,6-triisopropylphenyl.

Scheme 1 Synthesis of O-equatorial arylphosphoranes using the Martin ligand.

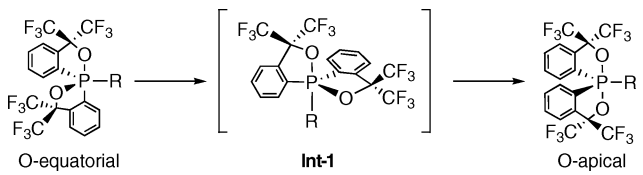

Scheme 2 High energy intermediate formed during the isomerization of the O-equatorial to O-apical isomer.

Theoretical studies have suggested that the π-donating substituents prefer to remain at the equatorial site of the TBP structure because such substituents are capable of interacting with the antibonding σ* orbitals.[8] Our group experimentally demonstrated that a dimethylamino group is less apicophilic than expected on the basis of its electronegativity, and this could be due to the existence of the $n_N \rightarrow \sigma^*_{P\text{-}C}$ interaction based upon the crystal structure of **7** (Fig. 2).[7a] By use of a pair of O-equatorial and O-apical benzylphosphoranes, we subsequently demonstrated that the O-equatorial α-carbanion **8** was less basic than the corresponding O-apical isomer **9**.[18] This result was supported by the density functional calculations showing that the $n_C \rightarrow \sigma^*_{P\text{-}O}$ interaction of the O-equatorial α-anion **8** was much greater than the $n_C \rightarrow \sigma^*_{P\text{-}C}$ interaction of the corresponding O-apical isomer **9**.[18] Moreover, based on the kinetic study of the isomerization of the O-equatorial aminophosphorane **10** to the O-apical isomer **11**, we succeeded in determining the energy of the $n_N \rightarrow \sigma^*_{P\text{-}O}$ interaction to be 4.4 kcal mol^{-1}, which was in good agreement with the calculated value (4.0 kcal mol^{-1}).[19]

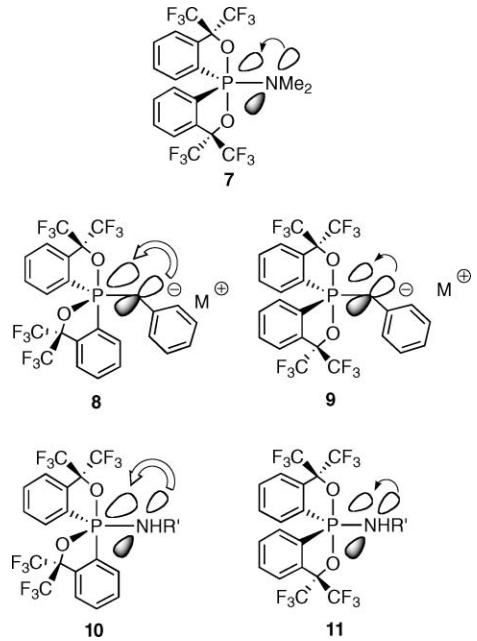

Fig. 2 The n → σ* interaction of the α-anions and aminophosphoranes.

Consequently, the interaction between the π-orbital of the monodentate aromatic ligand and the σ* orbital in the equatorial plane has been of significant interest. However, in the Martin ligand system (**A**), we isolated only the O-equatorial isomer with a TIP group (**5c**) as described above. Therefore, no insights into the π → σ* interaction were established in the study. Thus, if the O-equatorial isomer (**12**) bearing an *ortho*-unsubstituted aryl monodentate ligand could be prepared (Fig. 3), and if the *para*-substituents (X) of the monodentate ligand affect the rate of the isomerization of the O-equatorial (**12**) to O-apical (**13**) isomer, the $\pi \rightarrow \sigma^*_{P\text{-}O}$ interaction in the O-equatorial isomer (**12**) could be estimated.

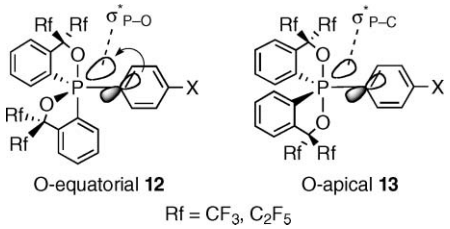

Fig. 3 Possible π → σ* interaction of arylphosphoranes.

In this context, we determined to employ the bulky bidentate ligand **B** for stabilizing the anti-apicophilic O-equatorial arylphosphoranes (**12**). We now report the isolation of O-equatorial arylphosphoranes **12** using ligand **B**. These O-equatorial phosphoranes, even the *ortho*-unsubstituted derivatives (**12a**–**d**), were found to be stable at r.t., and could still be converted into the O-apical isomer **13** at elevated temperatures. The structures of the O-equatorial phosphoranes as well as the O-apical isomers were unambiguously determined by an X-ray crystallographic analysis. The kinetic study furnished the activation parameters for the stereomutation of the O-equatorial arylphosphoranes **12** to the O-apical isomers **13**. Furthermore, the effect of the solvent and the *para*-substituent on the rate of the isomerization were also investigated in order to provide an insight into the $\pi \rightarrow \sigma^*_{P\text{-}O}$ interaction in the O-equatorial arylphosphoranes. Full details are given in the following sections.

Results and discussion

Synthesis and structure of the O-equatorial and O-apical arylphosphoranes

Using the new bidentate ligand **B**, the O-equatorial arylphosphoranes (**12**) were successfully synthesized by the reaction of the P–H spirophosphorane **14**[15a] with excess ArLi, followed by treatment with I_2 (Scheme 3).[17] All of the O-equatorial **12** was quantitatively converted into the corresponding O-apical isomers **13** by heating in an organic solvent. Considering the fact that the O-equatorial arylphosphoranes **5** except for **5c** (Ar = TIP) have not been isolated,[17] it is noted that even the *ortho*-unsubstituted derivatives (**12a**–**d**) are isolable using ligand **B**, indicating that the steric effect of the C_2F_5 groups for freezing the isomerization is also remarkable in the present case.

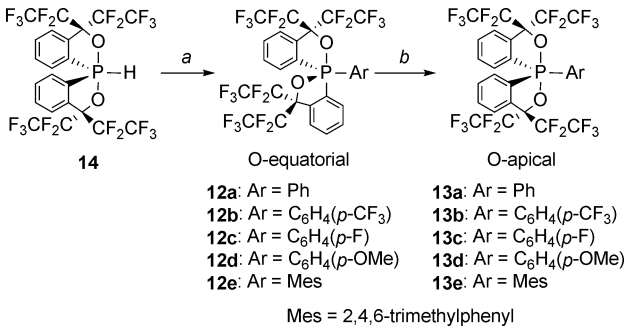

Scheme 3 Synthesis of the O-equatorial (**12**) and O-apical (**13**) arylphosphoranes. *Reagents and conditions*: (a) ArLi, Et_2O, r.t., 1 h, then I_2, −78 °C to 0 °C, 1 h, **12a**: 85%, **12b**: 58%, **12c**: 76%, **12d**: 48%, **12e**: 83%; (b) C_6D_6, 80 °C, 8 h, **13a**: 98%, **13b**: 96%, **13c**: 96%, **13d**: 97%, **13e**: 95%.

The structures of the O-equatorial (**12a**–**e**) and O-apical (**13d** and **13e**) phosphoranes were confirmed by an X-ray crystallographic analysis (Fig. 4). All compounds have a distorted trigonal-bipyramidal (TBP) structure, in which the aryl monodentate ligand occupies one of the equatorial sites. Two independent molecules were found in the unit cell for each of the **12a**, **12c** and **12e**. The angles and distances involving the phosphorus atom of **12** and **13** (Table 1) were similar to those of the corresponding alkylphosphoranes **3** and **4**, respectively. For the O-equatorial isomers, the equatorial O2–P–C1 angle of **12a**–**d** (**12a**: 120.5°, 124.0°; **12b**: 122.5°; **12c**: 121.7°, 124.1°; **12d**: 123.6°) is only slightly larger than those of the alkylphosphoranes (**3a**: 119.5°; **3b**: 119.7°; **3c**: 118.0°),[15a] although those of the mesityl derivative **12e** (112.8°,

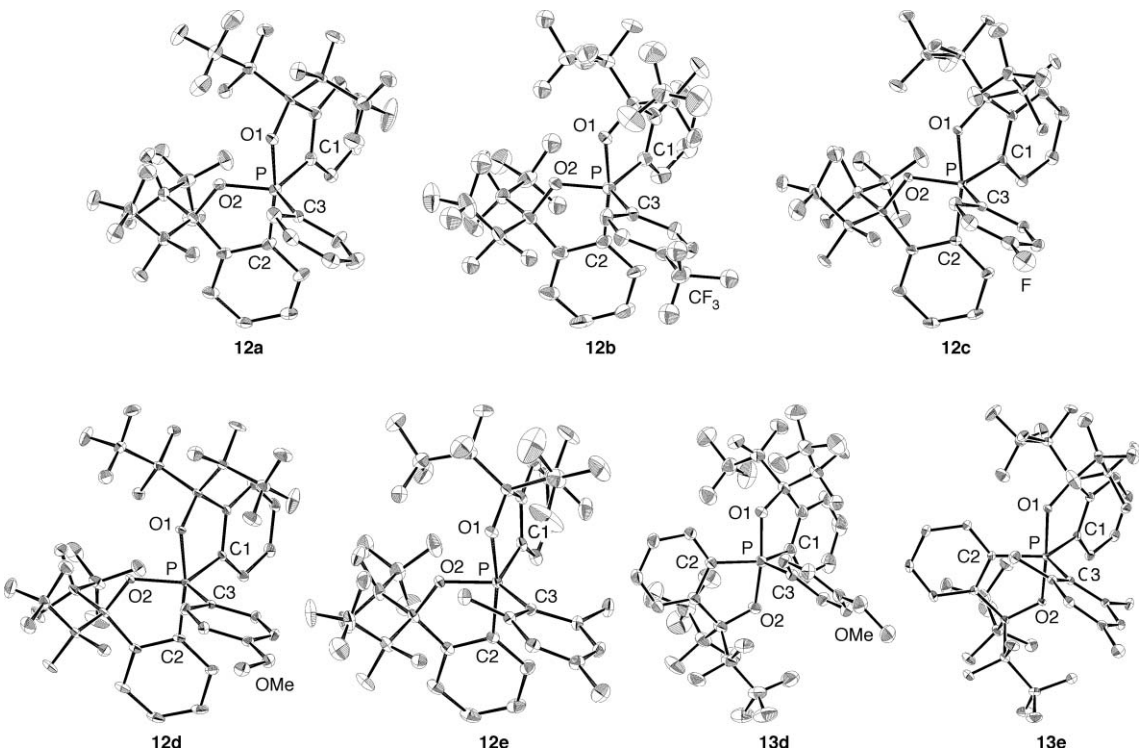

Fig. 4 ORTEP diagrams of arylphosphoranes with the thermal ellipsoids shown at the 30% probability level. For **12a**, **12c** and **12e**, one of the two independent molecules is shown. All hydrogen atoms are omitted for clarity.

Table 1 Selected bond lengths (Å) and angles (°) for the O-equatorial (**12**) and O-apical (**13**) phosphoranes

Compound	**12a**[a]	**12b**	**12c**[a]	**12d**	**12e**[a]	**13d**	**13e**
P–O1	1.775(4), 1.807(4)	1.788(5)	1.7870(12), 1.7800(12)	1.7742(14)	1.7781(19), 1.7845(18)	1.7435(13)	1.7663(10)
P–O2	1.666(5), 1.655(4)	1.643(5)	1.6501(12), 1.6564(12)	1.6654(13)	1.6636(18), 1.6722(18)	1.7526(13)	1.7663(10)
P–C1	1.824(7), 1.823(7)	1.813(7)	1.8215(17), 1.8229(17)	1.8264(17)	1.828(3), 1.817(3)	1.8335(18)	1.8298(15)
P–C2	1.889(6), 1.900(6)	1.878(7)	1.8805(17), 1.8763(18)	1.8810(19)	1.890(3), 1.887(3)	1.8294(17)	1.8282(14)
P–C3	1.825(6), 1.820(7)	1.841(7)	1.8245(17), 1.8191(17)	1.8125(18)	1.853(3), 1.850(2)	1.8045(18)	1.8422(15)
O1–P–O2	83.7(2), 81.32(19)	83.0(2)	82.26(6), 82.76(6)	82.34(6)	83.75(9), 82.60(9)	167.89(7)	174.02(5)
O1–P–C1	86.7(2), 86.6(2)	86.4(3)	87.06(7), 87.12(7)	86.95(7)	86.76(11), 87.12(10)	87.16(8)	86.85(6)
O1–P–C2	171.5(3), 168.6(2)	171.3(3)	170.13(7), 170.22(7)	169.59(8)	170.73(11), 169.61(10)	88.47(7)	90.68(6)
O1–P–C3	87.7(2), 89.5(2)	88.7(3)	89.17(7), 88.69(7)	89.20(7)	87.89(10), 88.06(10)	95.94(7)	93.52(6)
O2–P–C1	120.5(2), 124.0(2)	122.5(3)	121.70(7), 124.12(7)	123.63(7)	112.78(11), 115.18(10)	88.89(8)	90.28(6)
O2–P–C2	87.9(3), 87.3(2)	88.4(3)	87.97(7), 87.53(7)	87.25(8)	87.23(10), 87.14(10)	87.12(7)	86.72(6)
O2–P–C3	116.3(3), 116.9(3)	116.2(3)	118.47(7), 119.00(7)	117.75(7)	121.26(11), 125.08(11)	96.17(7)	92.46(6)
C1–P–C2	98.9(3), 99.4(3)	99.6(3)	99.32(8), 99.29(8)	99.12(8)	98.73(12), 98.81(11)	139.54(8)	125.52(7)
C1–P–C3	121.8(3), 117.4(3)	119.9(3)	118.48(8), 115.50(8)	117.24(8)	124.64(12), 118.23(11)	110.17(8)	118.85(6)
C2–P–C3	94.7(2), 96.2(3)	93.7(3)	94.32(7), 95.12(8)	95.43(8)	95.00(11), 96.52(11)	110.29(8)	115.63(7)

[a] Bond parameters for the two independent molecules are shown.

115.2°) are apparently smaller than those of **12a**–**d** and comparable to that of the O-equatorial TIP derivative **5c** (114.0°).[17] Similarly, for the O-apical phosphoranes, the equatorial C1–P–C2 angle of **13e** (125.5°) is smaller than that of **13d** (139.5°). This is mainly due to the steric repulsions between the bulky mesityl group and the aromatic rings of the bidentate ligand.

The degree of the tilt of the monodentate aryl ring can be represented by the tilt angle θ, which is the dihedral angle between the root mean plane consisting of P and the equatorial atoms (C1, O2 and C3 for **12**, C1, C2 and C3 for **13**) and that consisting of the six atoms of the monodentate aromatic ring (Fig. 5 and Table 2). For the *ortho*-unsubtituted O-equatorial derivatives (**12a**, **12b**, **12c** and **12d**), θ ranges from 14° to 33°, and the degree of the tilt is independent of the electronic property of the *para*-substituent. In addition, the two independent molecules for **12c** have different tilt angles (27.7° and 14.1°). This implies that the $\pi \rightarrow \sigma^*$ interactions in these arylphosphoranes are not strong enough to dominate the tilt angle of the crystal structure. Comparing the O-equatorial and O-apical isomers, the former has a smaller θ than the latter probably due to steric repulsions originating from the apical aromatic ring of the bidentate ligand. Overall, the crystal structures are mainly governed by steric reasons.

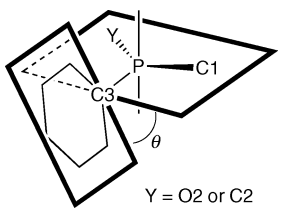

Fig. 5

Table 2 Tilt angles θ of phosphoranes

Compound	Ar	Y	θ/°
12a	Ph	O2	32.9, 29.8[a]
12b	C_6H_4(*p*-CF_3)	O2	24.4
12c	C_6H_4(*p*-F)	O2	27.7, 14.1[a]
12d	C_6H_4(*p*-OMe)	O2	18.8
12e	Mes	O2	24.8, 20.4[a]
13d	C_6H_4(*p*-OMe)	C2	42.6
13e	Mes	C2	34.0

[a] Tilt angles for the two independent molecules are shown.

Kinetic study of the isomerization of O-equatorial 12 to O-apical 13

The rates of the isomerization of **12** to **13** were measured by monitoring the change in the integrals of the ^{19}F NMR signals of the trifluoromethyl group, and the rates satisfied first-order kinetics. At first, in order to investigate the solvent effect for the isomerization, measurements of the stereomutation of **12a** to **13a** were carried out at 50 °C using DMSO-d_6, CD_3CN, MeOH and C_6D_6. The rates and solvent parameters (ε_r, μ and E_T^N)[20] are summarized in Table 3. The rates were found to be slightly affected by the polarity of the solvents, in which the polar solvent decelerated the isomerization.

In order to investigate the *p*-substituent effect, the rates of the isomerization for **12a–d** were then measured in C_6D_6 at 50 °C (Table 4). Although the rates of **12a–d** ((2.77, 3.77, 2.57 and 2.02) × 10^{-4} s^{-1} for **12a**, **12b**, **12c** and **12d**, respectively) were of the same order of magnitude, it was found that the stereomutation was decelerated by the electron-donating OMe group and accelerated by the electron-withdrawing CF_3 group. Table 4 shows the rate constants along with the substituent parameters (σ_p, σ_R and σ_I).[21] Although the isomerization rates (k) of **12** to **13** do not nicely correlate with each substituent parameter, the resonance

Table 3 The rates for the stereomutation from O-equatorial **12a** to O-apical **13a** in various solvents at 323 K

Solvent	ε_r[a]	$10^{30}\mu$[a]/C m	E_T^N[a]	k[b]/s^{-1}
DMSO-d_6	46.45	13.5	0.444	$(0.84 \pm 0.05) \times 10^{-4}$
CD_3CN	35.94	13.0	0.460	$(1.51 \pm 0.03) \times 10^{-4}$
MeOH	32.66	9.6	0.762	$(1.90 \pm 0.01) \times 10^{-4}$
C_6D_6	2.27	0.0	0.111	$(2.77 \pm 0.03) \times 10^{-4}$

[a] Values of undeuterated solvents are shown. [b] Error is given as the standard deviation.

Table 4 Effect of *p*-substituents on the isomerization rate in C_6D_6 at 323 K

Process	X	σ_p	σ_R	σ_I	$10^4 k/s^{-1}$
12a → 13a	H	0.00	0.00	0.00	2.77 ± 0.03
12b → 13b	CF_3	0.51	0.11	0.40	3.77 ± 0.03
12c → 13c	F	0.06	−0.48	0.54	2.57 ± 0.03
12d → 13d	OMe	−0.28	−0.58	0.30	2.02 ± 0.02

substituent parameter (σ_R) seemed to be a greater contribution than the inductive constant (σ_I). Thus, we carried out a multi-regression analysis using σ_R and σ_I as variants, and obtained the following equation with a very good fit of $R^2 = 0.996$.

$$k = (2.31\sigma_R + 1.72\sigma_I + 2.80) \times 10^{-4}$$

This equation shows that the contribution of the resonance effect on the isomerization rate is 1.3 times greater than that of the inductive effect. Since the $\sigma^*_{P\text{-}O}$ orbital of the O-equatorial phosphorane has found to be significantly lower in energy than the $\sigma^*_{P\text{-}C}$ orbital of the O-apical isomer,[18] the ground state (*i.e.*, TBP structure) of the O-equatorial *ortho*-unsubstituted derivatives (**12a–d**) should be somewhat stabilized by the $\pi \rightarrow \sigma^*_{P\text{-}O}$ interaction, whereas such an interaction can be negligible for the O-apical isomers (Fig. 3). In any case, this result agrees with the fact that the π-donating nature reduces the apparent apicophilicity of the substituent although the degree of the interaction is not significant.

The reason for the rather small interaction could be due to the small tilt angle described above (Fig. 5). Therefore, we investigated the structure in solution based on the ^{31}P and ^{19}F NMR. All the isolated phosphoranes showed singlets in ^{31}P NMR ($CDCl_3$), and the chemical shifts for the O-equatorial phosphoranes ($\delta = -10.6$ (**12a**), −11.4 (**12b**), −11.1 (**12c**), −10.7 (**12d**) and −2.6 (**12e**) ppm) were shifted downfield compared to those of the O-apical isomers ($\delta = -26.9$ (**13a**), −28.2 (**13b**), −27.7 (**13c**) and −27.1 (**13d**) and −23.6 (**13e**) ppm) similar to our previous results.[13,15,17–19] The ^{19}F NMR spectra of the O-apical phosphoranes (**13**) showed only two CF_3 signals due to their C_2 symmetrical structure. For the O-equatorial isomers, four CF_3 signals were observed for **12e** ($\delta = -78.1, -78.4, -79.1$ and −79.2 ppm) at room temperature or even at 60 °C, whereas there were only two CF_3 signals for **12a–d**. As we have already reported, for the O-equatorial phosphoranes bearing a bulky monodentate ligand (**5b** and **5c**), the four chemically nonequivalent CF_3 groups have been observed distinctly in the ^{19}F NMR. If a fast exchange between the $\boldsymbol{R}_P$* and $\boldsymbol{S}_P$* isomers takes place,[22] the two *endo*-CF_3 groups (*a-endo*-CF_3 and *b-endo*-CF_3) coalesce into one, and the same occurs for the *exo*-CF_3 groups (*a-exo*-CF_3 and *b-exo*-CF_3). Therefore, this observation implies that the one-step stereomutation between the $\boldsymbol{R}_P$* and $\boldsymbol{S}_P$* enantiomers of **12e** is slow on the NMR timescale (Scheme 4).

In the ^1H NMR, two kinds of *ortho*-methyl protons ($\delta = 2.65$ (s, 3H) and 2.27 ppm (s, 3H)) as well as *meta*-protons ($\delta = 6.81$ (d, $^4J_{H,P} = 4.4$ Hz, 1H), 6.73 ppm (d, $^4J_{H,P} = 8.3$ Hz, 1H)) were clearly observed for **12e**, whereas only a set of *ortho*- and *meta*-aromatic protons was observed for **12a–d**. That is, sites ***a*** and ***b*** of **12e** are not equivalent, whereas sites ***c*** and ***d*** of **12a–d** are equivalent in the ^1H NMR (Scheme 4). If the conformation of the monodentate ligand is fixed, sites ***a*** (or ***c***) and ***b*** (or ***d***) are not exchanged with each other upon the one-step pseudorotation

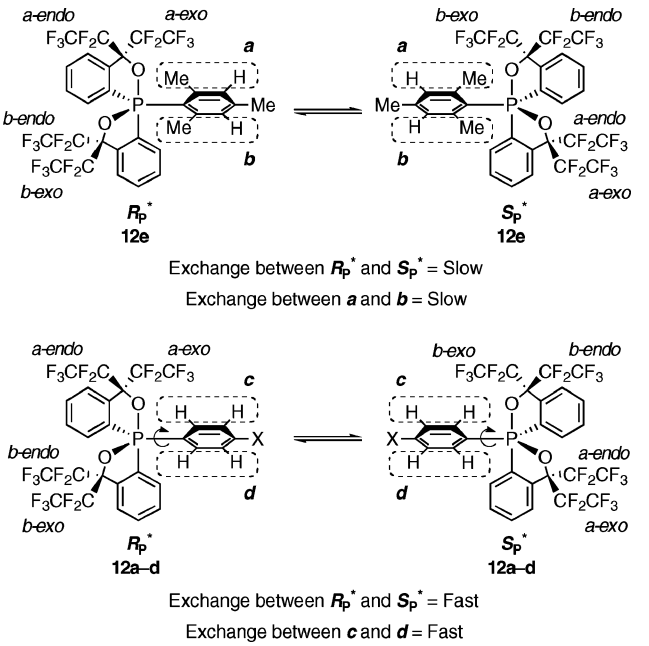

Scheme 4 Frozen one-step pseudorotation and P–C(*ipso*) rotation in the O-equatorial mesitylphophorane (**12e**)

between $\boldsymbol{R}_P$* and $\boldsymbol{S}_P$*. These observations indicate that the P–C(*ipso*) rotation in the mesityl derivative (**12e**) is slow and that in the *ortho*-unsubstituted derivatives (**12a–d**) is fast on the NMR timescale. Therefore, the degree of freedom in the P–C(*ipso*) bond rotation is higher for **12a–d** than for **12e** in the solution state. Thus, the *ortho*-unsubstituted aryl group of **12a–d** should be capable of being nearly perpendicular to the equatorial plane, whereas the mesityl group of **12e** is most likely fixed as the crystal structure even in solution. Therefore, the $\pi \rightarrow \sigma^*_{P\text{-}O}$ interaction should work well for the O-equatorial *ortho*-unsubstituted derivative (**12a–d**), giving rise to stabilization of the ground states of **12a–d**.

In order to investigate the difference between the *ortho*-unsubstituted aryl and mesityl groups, the rates of the isomerization of the phenyl (**12a** to **13a**) and the mesityl (**12e** to **13e**) derivatives were measured in the temperature range of 313–333 K (Table 5), and obtained the activation parameters from the Eyring plot (Fig. 6). The free energy of activation of the mesityl derivative

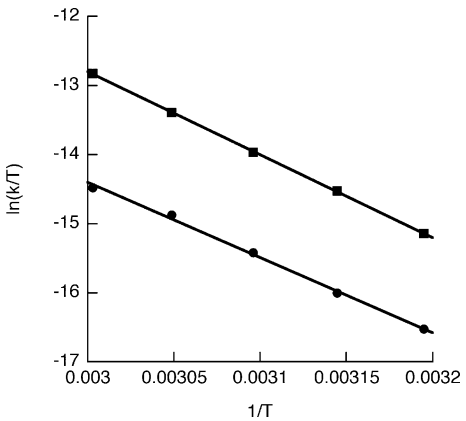

Fig. 6 Eyring plot for the isomerization in C_6D_6. Squares: **12a** → **13a**; circles: **12e** → **13e**.

Table 5 Activation parameters of the stereomutation in C_6D_6[a]

Process	T/K	k/s^{-1}	$\Delta H^{\ddagger}$/kcal mol^{-1}	$\Delta S^{\ddagger}$/cal K^{-1} mol^{-1}	$\Delta G^{\ddagger}_{298}$/kcal mol^{-1}
12a → **13a** (Ar = Ph)	313	$(0.81 \pm 0.01) \times 10^{-4}$	23.9 ± 0.2	−0.6 ± 0.6	24.1
	318	$(1.56 \pm 0.01) \times 10^{-4}$			
	323	$(2.77 \pm 0.03) \times 10^{-4}$			
	328	$(5.00 \pm 0.04) \times 10^{-4}$			
	333	$(8.96 \pm 0.10) \times 10^{-4}$			
12e → **13e** (Ar = Mes)	313	$(2.08 \pm 0.03) \times 10^{-5}$	21.6 ± 0.6	−10.8 ± 1.9	24.8
	318	$(3.56 \pm 0.02) \times 10^{-5}$			
	323	$(6.49 \pm 0.06) \times 10^{-5}$			
	328	$(11.3 \pm 0.03) \times 10^{-5}$			
	333	$(17.1 \pm 0.20) \times 10^{-5}$			

[a] Error is given as the standard deviation.

($\Delta G^{\ddagger}_{298}$ = 24.8 kcal mol^{-1}) is slightly higher than that of the phenyl derivative (24.1 kcal mol^{-1}). When compared to the CF_3 derivative, the free energy of activation for **12e** to **13e** ($\Delta G^{\ddagger}_{298}$ = 24.8 kcal mol^{-1}) was higher than that of **5b** to **6b** ($\Delta G^{\ddagger}_{298}$ = 22.2 kcal mol^{-1}) by 2.6 kcal mol^{-1}, and was comparable to that of the TIP derivative **5c** to **6c** ($\Delta G^{\ddagger}_{298}$ = 24.1 kcal mol^{-1}).[17b] This again proves the steric hindrance of the C_2F_5 group being more effective for freezing the isomerization than that of the CF_3 group.

As for the activation enthalpy ($\Delta H^{\ddagger}$) of the phenyl derivative (**12a** → **13a**) and of the mesityl derivative (**12e** → **13e**), the former is greater than the latter by 2.3 kcal mol^{-1} in clear contrast to the free energy of activation. When considering the high-energy intermediates in the three-step BPR from the O-equatorial **12** to the O-apical **13**,[13] the mesityl derivative (**Int-2e**) could be less stable than the phenyl derivative (**Int-2a**) because the former has a bulky mesityl group at the sterically congested apical site (Fig. 7). Therefore, the difference in enthalpy has to be explained by some factors in the ground state because the activation enthalpy is *lower* in the mesityl derivative (**12e** → **13e**) than in the phenyl derivative (**12a** → **13a**). The $\pi \rightarrow \sigma^*_{P\text{-}O}$ stabilizing interaction in **12a** can be one of the reasons for the higher activation enthalpy for **12a** → **13a**. The activation entropy ($\Delta S^{\ddagger}$) for the mesityl derivative (**12e** → **13e**) is *lower* than that for the phenyl derivative (**12a** → **13a**). The steric repulsion between the bulky mesityl group and the bidentate ligands even in **Int-2e** could be the reason.

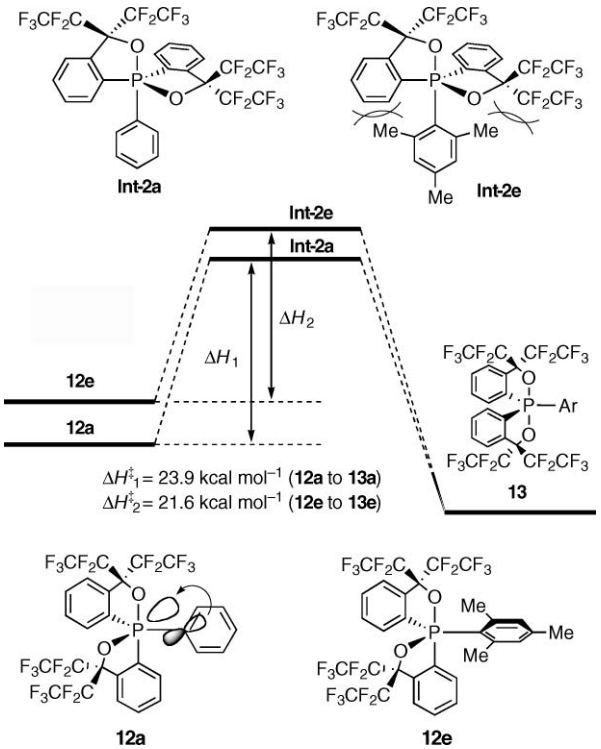

Fig. 7 Energy diagram for the isomerization of the O-equatorial phosphoranes to the O-apical isomers.

Conclusions

The new bidentate ligand with two C_2F_5 groups was used to isolate the O-equatorial arylphosphoranes **12** (Ar = Ph, C_6H_4(*p*-CF_3), C_6H_4(*p*-F), C_6H_4(*p*-OMe) and Mes), which could be quantitatively converted into the corresponding O-apical isomers **13** by heating at elevated temperatures. The structures were confirmed by an X-ray analysis, showing that the tilt angle of the monodentate ligand was found to be independent of the *para*-substituents. However, the kinetic study showed a small *para*-substituent effect on the stereomutations. The multi-regression analysis for the *para*-substituents revealed that the contribution of the resonance effect (σ_R) on the rate constant was superior to the inductive effect (σ_I). This indicates that the $\pi \rightarrow \sigma^*_{P\text{-}O}$ stabilizing interaction in the O-equatorial isomer plays some role in the isomerization. This result shows a general insight into the stereoelectronic effect of the pentacoordinated molecules.

Experimental

General

Melting points were measured using a Yanaco micro melting point apparatus. The ^{1}H NMR (400 MHz), ^{19}F NMR (376 MHz), ^{31}P NMR (162 MHz) were recorded using JEOL EX-400 or JEOL AL-400 spectrometers. The ^{1}H NMR chemical shifts (δ) are given in ppm downfield from Me_4Si, determined by residual chloroform (δ = 7.26 ppm). The ^{19}F NMR chemical shifts are given in ppm downfield from the external $CFCl_3$. The ^{31}P NMR chemical shifts are given in ppm downfield from the external 85% H_3PO_4. The elemental analyses were performed using a Perkin-Elmer 2400 CHN elemental analyzer. All reactions were carried out under N_2. Diethyl ether (Et_2O) was freshly distilled from Na/benzophenone,

and the other solvents were distilled from CaH_2. Merck silica gel $60GF_{254}$ was used for the preparative thin-layer chromatography.

General procedure for the synthesis of O-equatorial arylphosphoranes

Synthesis of 12a. PhLi (1.14 M cyclohexane–Et_2O solution, 0.19 mL, 0.216 mmol) was added to a solution of P–H phosphorane **14** (49.9 mg, 0.0696 mmol) in Et_2O (3.0 mL) at −78 °C. The mixture was then stirred for 1 h at room temperature. I_2 (52.0 mg, 0.204 mmol) was added to the mixture at −78 °C, and the mixture was stirred for 1 h at 0 °C. The reaction was then quenched with aqueous $Na_2S_2O_3$ (30 mL). The mixture was extracted with Et_2O (2 × 40 mL), and the organic layer was washed with brine (2 × 40 mL) and dried over anhydrous $MgSO_4$. After removing the solvents by evaporation, the resulting crude product was separated by preparative TLC (*n*-hexane–CH_2Cl_2 = 7 : 1) to afford **12a** (47.0 mg, 0.0593 mmol, 85%) as a white solid. Colorless crystals of **12a** suitable for the X-ray analysis were obtained by recrystallization from *n*-hexane–CH_2Cl_2. Mp 115.0–116.0 °C (decomp.). ^{1}H NMR (400 MHz, $CDCl_3$): δ = 7.95–7.99 (m, 2 H, Ar–H), 7.74 (br s, 2 H, Ar–H), 7.59–7.62 (m, 4 H, Ar–H), 7.49–7.55 (m, 2 H, Ar–H), 7.24–7.28 (m, 3 H, Ar–H) ppm. ^{19}F NMR (376 MHz, $CDCl_3$): δ −78.8 (s, 6 F, CF_2CF_3), −79.4 (dd, $^3J_{F,F}$ = 9.8 Hz, $^5J_{F,F}$ = 9.8 Hz, 6 F, CF_2CF_3), −114.8 (d, $^2J_{F,F}$ = 295.6 Hz, 2 F, CF_2CF_3), −116.1 (d, $^2J_{F,F}$ = 295.6 Hz, 4 F, CF_2CF_3), −118.4 (dm, $^2J_{F,F}$ = 295.6 Hz, 2 F, CF_2CF_3) ppm. ^{31}P NMR (162 MHz, $CDCl_3$): δ −10.6 ppm. Anal. Found: C, 42.43; H, 1.26. Calc. for $C_{28}H_{13}F_{20}O_2P$: C, 42.44; H, 1.65%.

Synthesis of 12b. Following the above-described procedure using *p*-bromobenzotrifluoride (d = 1.607 g mL^{-1}, 0.040 mL, 0.29 mmol) and **14** (51.8 mg, 0.0723 mmol), **12b** (36.0 mg, 0.0418 mmol, 58%) was isolated as a white solid. Colorless crystals of **12b** suitable for the X-ray analysis were obtained by recrystallization from *n*-hexane–CH_2Cl_2. Mp 106.0–107.0 °C (decomp.). ^{1}H NMR (400 MHz, $CDCl_3$): δ 7.92–7.96 (m, 2 H, Ar–H), 7.76 (br s, 2 H, Ar–H), 7.62–7.66 (m, 4 H, Ar–H), 7.61 (dd, $^3J_{H,P}$ = 15.0 Hz, $^3J_{H,H}$ = 8.3 Hz, 2 H, Ar–H), 7.53 (d, $^4J_{H,P}$ = 7.8 Hz, $^3J_{H,H}$ = 8.3 Hz, 2 H, Ar–H) ppm. ^{19}F NMR (376 MHz, $CDCl_3$): δ −63.5 (s, 3 F, Ar–CF_3), −78.8 (s, 6 F, CF_2CF_3), −79.5 (dd, $^3J_{F,F}$ = 9.8 Hz, $^5J_{F,F}$ = 9.8 Hz, 6 F, CF_2CF_3), −114.8 (d, $^2J_{F,F}$ = 292.0 Hz, 2 F, CF_2CF_3), −116.2 (br dm, $^2J_{F,F}$ = 292.0 Hz, 4 F, CF_2CF_3), −118.4 (dm, $^2J_{F,F}$ = 292.0 Hz, 2 F, CF_2CF_3) ppm. ^{31}P NMR (162 MHz, $CDCl_3$): δ −11.4 ppm. Anal. Found: C, 40.19; H, 1.01. Calc. for $C_{29}H_{12}F_{23}O_2P$: C, 40.49; H, 1.41%.

Synthesis of 12c. Following the above-described procedure using *p*-bromofluorobenzene (d = 1.593 g mL^{-1}, 0.040 mL, 0.36 mmol) and **14** (47.7 mg, 0.0665 mmol), **12c** (41.2 mg, 0.0508 mmol, 76%) was isolated as a white solid. Colorless crystals of **12c** suitable for the X-ray analysis were obtained by recrystallization from *n*-hexane–CH_2Cl_2. Mp 112.5–113.5 °C (decomp.). ^{1}H NMR (400 MHz, $CDCl_3$): δ 7.93–7.98 (m, 2 H, Ar–H), 7.76 (br d, $^3J_{H,H}$ = 8.0 Hz, 2 H, Ar–H), 7.61–7.64 (m, 4 H, Ar–H), 7.54 (ddd, $^3J_{H,P}$ = 15.0 Hz, $^3J_{H,H}$ = 9.0 Hz, $^4J_{H,F}$ = 6.0 Hz, 2 H, Ar–H), 6.96 (ddd, $^3J_{H,F}$ = 9.0 Hz, $^3J_{H,H}$ = 9.0 Hz, $^4J_{H,P}$ = 3.6 Hz, 2 H, Ar–H) ppm. ^{19}F NMR (376 MHz, $CDCl_3$): δ −78.8 (s, 6 F, CF_2CF_3), −79.5 (dd, $^3J_{F,F}$ = 9.8 Hz, $^5J_{F,F}$ = 9.8 Hz, 6 F, CF_2CF_3), −111.0 (tt, $^3J_{H,F}$ = 9.0 Hz, $^4J_{H,F}$ = 6.0 Hz, 1 F, Ar-F), −114.9 (d, $^2J_{F,F}$ = 292.0 Hz, 2 F, CF_2CF_3), −116.1 (d, $^2J_{F,F}$ = 292.0 Hz, 4 F, CF_2CF_3), −118.5 (dm, $^2J_{F,F}$ = 292.0 Hz, 2 F, CF_2CF_3) ppm. ^{31}P NMR (162 MHz, $CDCl_3$): δ −11.1 ppm. Anal. Found: C, 41.48; H, 1.18. Calc. for $C_{28}H_{12}F_{21}O_2P$: C, 41.50; H, 1.49%.

Synthesis of 12d. Following the above-described procedure using *p*-bromoanisole (d = 1.494 g mL^{-1}, 0.060 mL, 0.48 mmol) and **14** (62.5 mg, 0.0872 mmol), **12d** (34.7 mg, 0.0421 mmol, 48%) was isolated as a white solid. Colorless crystals of **12d** suitable for the X-ray analysis were obtained by recrystallization from *n*-hexane–CH_2Cl_2. Mp 124.0–125.0 °C (decomp.). ^{1}H NMR (400 MHz, $CDCl_3$): δ 7.96–8.03 (m, 2 H, Ar–H), 7.76 (br s, 2 H, Ar–H), 7.58–7.61 (m, 4 H, Ar–H), 7.50 (dd, $^3J_{H,P}$ = 15.0 Hz, $^3J_{H,H}$ = 8.8 Hz, 2 H, Ar–H), 6.78 (d, $^4J_{H,P}$ = 7.8 Hz, $^3J_{H,H}$ = 8.8 Hz, 2 H, Ar–H), 3.74 (s, 3 H, Ar-OCH_3) ppm. ^{19}F NMR (376 MHz, $CDCl_3$): δ −78.8 (s, 6 F, CF_2CF_3), −79.4 (dd, $^3J_{F,F}$ = 9.8 Hz, $^5J_{F,F}$ = 9.8 Hz, 6 F, CF_2CF_3), −115.0 (d, $^2J_{F,F}$ = 292.0 Hz, 2 F, CF_2CF_3), −116.2 (br d, $^2J_{F,F}$ = 292.0 Hz, 4 F, CF_2CF_3), −118.5 (dm, $^2J_{F,F}$ = 292.0 Hz, 2 F, CF_2CF_3) ppm. ^{31}P NMR (162 MHz, $CDCl_3$): δ −10.7 ppm. Anal. Found: C, 42.05; H, 1.60. Calc. for $C_{29}H_{15}F_{20}O_3P$: C, 42.35; H, 1.84%.

Synthesis of 12e. Following the above-described procedure using 2-bromomesitylene (d = 1.301 g mL^{-1}, 0.10 mL, 0.65 mmol) and **14** (71.3 mg, 0.0995 mmol), **12e** (69.2 mg, 0.0829 mmol, 83%) was isolated as a white solid. Colorless crystals of **12e** suitable for the X-ray analysis were obtained by recrystallization from CH_3CN. Mp 113.1–113.9 °C. ^{1}H NMR (400 MHz, $CDCl_3$): δ 7.95–7.98 (m, 1 H, Ar–H), 7.81 (br d, $^3J_{H,H}$ = 8.0 Hz, 1 H, Ar–H), 7.69 (td, $^3J_{H,H}$ = 8.0 Hz, $^4J_{H,H}$ = 1.2 Hz, 1 H, Ar–H), 7.61 (br d, $^3J_{H,H}$ = 8.0 Hz, 1 H, Ar–H), 7.44–7.53 (m, 4 H, Ar–H), 6.81 (d, $^4J_{H,P}$ = 4.4 Hz, 1 H, Ar–H), 6.73 (d, $^4J_{H,P}$ = 8.3 Hz, 1 H, Ar–H), 2.65 (s, 3 H, Ar–CH_3), 2.27 (s, 3 H, Ar–CH_3), 2.18 (s, 3 H, Ar–CH_3) ppm. ^{19}F NMR (376 MHz, $CDCl_3$): δ −78.1 (s, 3 F, CF_2CF_3), −78.4 (s, 3 F, CF_2CF_3), −79.1 (s, 3 F, CF_2CF_3), −79.2 (s, 3 F, CF_2CF_3), −112.9 (d, $^2J_{F,F}$ = 292.0 Hz, 1 F, CF_2CF_3), −113.8 (d, $^2J_{F,F}$ = 292.0 Hz, 1 F, CF_2CF_3), −114.1 (d, $^2J_{F,F}$ = 292.0 Hz, 2 F, CF_2CF_3), −114.9 (d, $^2J_{F,F}$ = 292.0 Hz, 1 F, CF_2CF_3), −115.3 (d, $^2J_{F,F}$ = 292.0 Hz, 1 F, CF_2CF_3), −115.7 (d, $^2J_{F,F}$ = 292.0 Hz, 1 F, CF_2CF_3), −117.8 (d, $^2J_{F,F}$ = 292.0 Hz, 1 F, CF_2CF_3) ppm. ^{31}P NMR (162 MHz, $CDCl_3$): δ −2.7 ppm. Anal. Found: C, 44.54; H, 2.07. Calc. for $C_{31}H_{19}F_{20}O_2P$: C, 44.62; H, 2.30%.

Synthesis of 13a. A solution of **12a** (12.2 mg, 0.0153 mmol) in C_6D_6 (1.0 mL) was heated at 80 °C for 8 h. After concentration *in vacuo*, **13a** was obtained (12.0 mg, 0.0151 mmol, 98%) as a white solid. Mp 149.1–150.0 °C. ^{1}H NMR (400 MHz, $CDCl_3$): δ 8.70–8.78 (m, 2 H, Ar–H), 7.69–7.82 (m, 6 H, Ar–H), 7.41 (dd, $^3J_{H,P}$ = 15.8 Hz, $^3J_{H,H}$ = 8.0 Hz, 2 H, Ar–H), 7.18–7.27 (m, 3 H, Ar–H) ppm. ^{19}F NMR (376 MHz, $CDCl_3$): δ −78.3 (s, 6 F, CF_2CF_3), −79.8 (dd, $^3J_{F,F}$ = 19.7 Hz, $^5J_{F,F}$ = 6.2 Hz, 6 F, CF_2CF_3), −116.7 (s, 2 F, CF_2CF_3), −116.8 (s, 2 F, CF_2CF_3), −116.8 (dq, $^2J_{F,F}$ = 285.8 Hz, $^3J_{F,F}$ = 19.7 Hz, 2 F, CF_2CF_3), −121.9 (dq, $^2J_{F,F}$ = 285.8 Hz, $^5J_{F,F}$ = 6.2 Hz, 2 F, CF_2CF_3) ppm. ^{31}P NMR (162 MHz, $CDCl_3$): δ −26.9 ppm. Anal. Found: C, 42.30; H, 1.64. Calc. for $C_{28}H_{13}F_{20}O_2P$: C, 42.44; H, 1.65%.

Synthesis of 13b. A solution of **12b** (14.0 mg, 0.0162 mmol) in C_6D_6 (1.0 mL) was heated at 80 °C for 8 h. After concentration *in vacuo*, **13b** was obtained (13.5 mg, 0.0157 mmol, 96%) as a

white solid. Mp 115.0–116.0 °C. ^{1}H NMR (400 MHz, $CDCl_3$): δ 8.69–8.74 (m, 2 H, Ar–H), 7.71–7.84 (m, 6 H, Ar–H), 7.51 (dd, $^3J_{H,P}$ = 15.4 Hz, $^3J_{H,H}$ = 8.0 Hz, 2 H, Ar–H), 7.45 (dd, $^4J_{H,P}$ = 7.6 Hz, $^3J_{H,H}$ = 8.0 Hz, 2 H, Ar–H) ppm. ^{19}F NMR (376 MHz, $CDCl_3$): δ −63.5 (s, 3 F, Ar–CF_3), −78.2 (s, 6 F, CF_2CF_3), −79.9 (dd, $^3J_{F,F}$ = 19.7 Hz, $^5J_{F,F}$ = 6.2 Hz, 6 F, CF_2CF_3), −116.7 (s, 2 F, CF_2CF_3), −116.8 (s, 2 F, CF_2CF_3), −116.8 (dq, $^2J_{F,F}$ = 285.8 Hz, $^3J_{F,F}$ = 19.7 Hz, 2 F, CF_2CF_3), −121.8 (dq, $^2J_{F,F}$ = 285.8 Hz, $^5J_{F,F}$ = 6.2 Hz, 2 F, CF_2CF_3) ppm. ^{31}P NMR (162 MHz, $CDCl_3$): δ −28.2 ppm. Anal. Found: C, 40.13; H, 1.07. Calc. for $C_{29}H_{12}F_{23}O_2P$: C, 40.49; H, 1.41%.

Synthesis of 13c. A solution of **12c** (11.8 mg, 0.0145 mmol) in C_6D_6 (1.0 mL) was heated at 80 °C for 8 h. After concentration *in vacuo*, **13c** was obtained (11.4 mg, 0.0140 mmol, 96%) as a white solid. Mp 120.0–121.0 °C. ^{1}H NMR (400 MHz, $CDCl_3$): δ 8.67–8.72 (m, 2 H, Ar–H), 7.71–7.83 (m, 6 H, Ar–H), 7.37–7.45 (m, 2 H, Ar–H), 6.84–6.91 (m, 2 H, Ar–H) ppm. ^{19}F NMR (376 MHz, $CDCl_3$): δ −78.3 (s, 6 F, CF_2CF_3), −79.8 (dd, $^3J_{F,F}$ = 19.7 Hz, $^5J_{F,F}$ = 6.2 Hz, 6 F, CF_2CF_3), −110.2 to −110.3 (m, 1 F, Ar–F), −116.7 (s, 2 F, CF_2CF_3), −116.8 (s, 2 F, CF_2CF_3), −116.8 (dq, $^2J_{F,F}$ = 285.8 Hz, $^3J_{F,F}$ = 19.7 Hz, 2 F, CF_2CF_3), −121.8 (dq, $^2J_{F,F}$ = 285.8 Hz, $^5J_{F,F}$ = 6.2 Hz, 2 F, CF_2CF_3) ppm. ^{31}P NMR (162 MHz, $CDCl_3$): δ −27.7 ppm. Anal. Found: C, 41.37; H, 1.33. Calc. for $C_{28}H_{12}F_{21}O_2P$: C, 41.50; H, 1.49%.

Synthesis of 13d. A solution of **12d** (12.1 mg, 0.0147 mmol) in C_6D_6 (1.0 mL) was heated at 80 °C for 8 h. After concentration *in vacuo*, **13d** was obtained (11.8 mg, 0.0143 mmol, 97%) as a white solid. Colorless crystals of **13d** suitable for the X-ray analysis were obtained by recrystallization from *n*-hexane–CH_2Cl_2. Mp 117.0–117.8 °C. ^{1}H NMR (400 MHz, $CDCl_3$): δ 8.68–8.72 (m, 2 H, Ar–H), 7.67–7.78 (m, 6 H, Ar–H), 7.38 (dd, $^3J_{H,P}$ = 15.2 Hz, $^3J_{H,H}$ = 8.8 Hz, 2 H, Ar–H), 6.69 (dd, $^4J_{H,P}$ = 3.4 Hz, $^3J_{H,H}$ = 8.8 Hz, 2 H, Ar–H), 3.73 (s, 3 H, Ar–OCH_3) ppm. ^{19}F NMR (376 MHz, $CDCl_3$): δ −78.3 (s, 6 F, CF_2CF_3), −79.7 (dd, $^3J_{F,F}$ = 19.7 Hz, $^5J_{F,F}$ = 6.2 Hz, 6 F, CF_2CF_3), −116.7 (s, 2 F, CF_2CF_3), −116.8 (s, 2 F, CF_2CF_3), −116.8 (dq, $^2J_{F,F}$ = 285.8 Hz, $^3J_{F,F}$ = 19.7 Hz, 2 F, CF_2CF_3), −121.8 (dq, $^2J_{F,F}$ = 285.8 Hz, $^5J_{F,F}$ = 6.2 Hz, 2 F, CF_2CF_3) ppm. ^{31}P NMR (162 MHz, $CDCl_3$): δ −27.1 ppm. Anal. Found: C, 42.27; H, 1.46. Calc. for $C_{29}H_{15}F_{20}O_3P$: C, 42.35; H, 1.84%.

Synthesis of 13e. A solution of **12e** (21.6 mg, 0.0258 mmol) in C_6D_6 (2.0 mL) was heated at 80 °C for 8 h. After concentration *in vacuo*, **13e** was obtained (20.5 mg, 0.0245 mmol, 95%) as a white solid. Colorless crystals of **13e** suitable for the X-ray analysis were obtained by recrystallization from *n*-hexane/CH_2Cl_2. 190.0–191.0 °C. ^{1}H NMR (400 MHz, $CDCl_3$): δ 8.56–8.61 (m, 2 H, Ar–H), 7.73 (br s, 2 H, Ar–H), 7.66–7.71 (m, 4 H, Ar–H), 6.58 (d, $^4J_{H,P}$ = 6.2 Hz, 2 H, Ar–H), 2.15 (s, 3 H, Ar-CH_3), 2.00 (s, 6 H, Ar–CH_3) ppm. ^{19}F NMR (376 MHz, $CDCl_3$): δ −77.0 (s, 6 F, CF_2CF_3), −79.7 (dd, $^3J_{F,F}$ = 16.0 Hz, $^5J_{F,F}$ = 8.6 Hz, 6 F, CF_2CF_3), −114.6 (dq, $^2J_{F,F}$ = 284.6 Hz, $^3J_{F,F}$ = 16.0 Hz, 2 F, CF_2CF_3), −115.9 (dd, $^2J_{F,F}$ = 284.6 Hz, $^4J_{F,F}$ = 33.2 Hz, 2 F, CF_2CF_3), −116.94 (d, $^2J_{F,F}$ = 284.6 Hz, 1 F, CF_2CF_3), −116.97 (d, $^2J_{F,F}$ = 284.6 Hz, 1 F, CF_2CF_3), −118.1 (ddq, $^2J_{F,F}$ = 284.6 Hz, $^4J_{F,F}$ = 33.2 Hz, $^5J_{F,F}$ = 8.6 Hz, 2 F, CF_2CF_3) ppm. ^{31}P NMR (162 MHz, $CDCl_3$): δ −23.6 ppm. Anal. Found: C, 44.47; H, 1.96. Calc. for $C_{31}H_{19}F_{20}O_2P$: C, 44.62; H, 2.30%.

Table 6 Crystallographic data

Compound	**12a**	**12b**	**12c**	**12d**	**12e**·0.5CH_3CN	**13d**	**13e**
Formula	$C_{28}H_{13}F_{20}O_2P$	$C_{29}H_{12}F_{23}O_2P$	$C_{28}H_{12}F_{21}O_2P$	$C_{29}H_{15}F_{20}O_3P$	$C_{32}H_{20.5}F_{20}N_{0.5}O_2P$	$C_{29}H_{15}F_{21}O_3P$	$C_{31}H_{19}F_{20}O_2P$
M_r	792.35	860.36	810.35	822.38	854.96	822.38	834.43
Crystal system	Monoclinic	Monoclinic	Triclinic	Triclinic	Triclinic	Monoclinic	Triclinic
Space group	$P2_1/n$	$P2_1/c$	$P\bar{1}$	$P\bar{1}$	$P\bar{1}$	$P2_1/c$	$P\bar{1}$
Color	Colorless	Colorless	Colorless	Colorless	Colorless	Colorless	Colorless
Habit	Plate	Plate	Plate	Plate	Plate	Plate	Plate
Crystal dimensions/mm	0.50 × 0.06 × 0.06	0.50 × 0.10 × 0.10	0.50 × 0.40 × 0.20	0.50 × 0.10 × 0.10	0.60 × 0.40 × 0.40	0.60 × 0.60 × 0.40	0.40 × 0.30 × 0.30
a/Å	9.6370(2)	10.3050(3)	8.94800(10)	9.25000(10)	11.11300(10)	9.8670(2)	9.9960(2)
b/Å	37.4070(13)	18.2210(6)	16.9750(3)	9.7100(2)	15.5850(3)	17.2000(3)	11.9660(3)
c/Å	16.1350(8)	16.8820(4)	19.6870(4)	18.0170(5)	19.1520(4)	18.8740(3)	14.1910(3)
α/°	90	90	88.1130(10)	84.9520(10)	97.5780(10)	90	86.9670(10)
β/°	96.6920(10)	95.292(3)	82.1650(10)	77.0590(10)	97.1530(10)	101.8580(10)	87.4260(10)
γ/°	90	90	81.3020(10)	72.817(2)	95.4110(10)	90	68.0970(10)
V/Å^3	5776.9(4)	3156.38(16)	2928.09(9)	1506.33(5)	3241.75(10)	3134.80(10)	1572.10(6)
Z	8	4	4	2	4	4	2
D_c/g cm^{-3}	1.822	1.810	1.838	1.813	1.752	1.742	1.763
μ/mm^{-1}	0.254	0.254	0.258	0.250	0.234	0.240	0.238
F(000)	3136	1696	1600	816	1708	1632	832
Radiation; λ/Å	Mo-Kα, 0.71073	Mo-Kα, 0.71073	Mo-Kα, 0.71073	Mo-Kα, 0.71073	Mo-Kα, 0.71073	Mo-Kα, 0.71073	Mo-Kα, 0.71073
T/K	173	293	173	173	200	293	173
Data collected	$+h, +k, \pm l$	$+h, +k, \pm l$	$+h, \pm k, \pm l$	$+h, \pm k, \pm l$	$+h, \pm k, \pm l$	$+h, +k, \pm l$	$+h, \pm k, \pm l$
Data/restraints/parameters	9091/0/919	6824/0/497	12473/0/937	6580/0/479	13990/0/1007	7443/0/479	6952/0/490
R_1 ($I > 2\sigma(I)$)	0.0839	0.1149	0.0415	0.0421	0.0705	0.0486	0.0352
wR_2 (all data)	0.2914	0.3878	0.1196	0.1480	0.2089	0.1689	0.1256
GOF	1.118	1.109	1.076	1.114	1.036	1.153	1.126

Single-crystal X-ray analyses of 12a, 12b, 12c, 12d, 12e, 13d and 13e

Crystals suitable for the X-ray structural determination were mounted on a Mac Science DIP2030 imaging plate diffractometer and irradiated with graphite monochromated Mo-Kα radiation ($\lambda = 0.71073$ Å) for the data collection. The unit cell parameters were determined by separately autoindexing several images in each data set using the DENZO program (MAC Science).[23] For each data set, the rotation images were collected in 3° increments with a total rotation of 180° about the ϕ axis. The data were processed using SCALEPACK. The structure was solved by a direct method using the SHELXS-97 program.[24] Refinement on F^2 was carried out using a full-matrix least-squares by the SHELXL-97 program.[24] All non-hydrogen atoms were refined using the anisotropic thermal parameters. The hydrogen atoms were included in the refinement along with isotropic thermal parameters. The crystallographic data are summarized in Table 6.

CCDC reference numbers 672351 (**12a**), 672352 (**12b**), 672353 (**12c**), 672354 (**12d**), 672355 (**12e**), 672356 (**13d**) and 672357 (**13e**).

For crystallographic data in CIF or other electronic format see DOI: 10.1039/b802947d

Kinetic measurements of the isomerization of 12 to 13

Samples (*ca.* 5 mg) in C_6D_6 (0.6 mL) were sealed in an NMR tube under N_2. Kinetic measurements of the pseudorotation process were carried out using a JEOL EX-400 spectrometer by monitoring the ^{19}F NMR signals in a variable temperature mode, and the specified temperatures were maintained throughout each set of measurements (error within ±1 °C). The observed temperatures were calibrated with the ^{19}F NMR chemical shift difference in the signals of neat 1,3-propanediol (high temperature region) and MeOH (low temperature region). The data were analyzed on the basis of the first-order kinetics using the following equation: $\ln(C_0/C_{12}) = kT$, in which C_0 = ratio of **12** at $t = 0$, C_{12} = ratio of **12** at arbitrary intervals. Here $C_0 = C_{12} + C_{13}$, $C_0/C_{12} = (C_{12} + C_{13})/C_{12} = 1 + C_{13}/C_{12}$. The C_{13}/C_{12} ratio was monitored by the integration of the ^{19}F NMR signals of the trifluoromethyl group at 40–60 °C. The rate constants and activation parameters for the stereomutation from **12** to **13** are shown in Tables 3–5.

Acknowledgements

The authors are grateful to Central Glass Co., Ltd., for the generous gift of the *p*-bromobenzotrifluoride. This work was supported by two Grants-in-Aid for Scientific Research on Priority Areas (Nos. 14340199, 17350021) from the Ministry of Education, Culture, Sports, Science and Technology, Japan.

References

1 (*a*) K.-y. Akiba, *Chemistry of Hypervalent Compounds*, Wiley-VCH, New York, 1999; (*b*) R. R. Holmes, *Pentacoordinated Phosphorus - Structure and Spectroscopy*, ACS Monographs 175, 176, vol, I, II; American Chemical Society, Washington, DC, 1980; (*c*) D. E. C. Corbridge, *Phosphorus: An Outline of Its Chemistry, Biochemistry, and Technology*, Elsevier, Amsterdam, 4th edn, 1990, ch. 14, pp. 1233–1256; (*d*) R. Burgada and R. Setton, in *The Chemistry of Organophosphorus Compounds*, ed. F. R. Hartley, Wiley-Interscience, Chichester, UK, 1994, vol. 3, pp. 185–277.

2 For the *N*-X-*L* designation, see: C. W. Perkins, J. C. Martin, A. J. Arduengo, W. Lau, A. Alegria and J. K. Kochi, *J. Am. Chem. Soc.*, 1980, **102**, 7753–7759.

3 (*a*) A. C. Hengge, *Acc. Chem. Res.*, 2002, **35**, 105–112, and references therein; (*b*) S. D. Lahiri, G. Zhang, D. Dunaway-Mariano and K. N. Allen, *Science.*, 2003, **299**, 2067–2071; (*c*) R. R. Holmes, *Acc. Chem. Res.*, 2004, **37**, 746–753; (*d*) F. H. Westheimer, *Acc. Chem. Res.*, 1968, **1**, 70–78; (*e*) G. R. J. Thatcher and R. Kluger, *Adv. Phys. Org. Chem.*, 1989, **25**, 99–265; (*f*) for recent mechanistic studies on phosphoryl transfer reaction, see: C. S. López, O. N. Faza, A. R. de Lera and D. M. York, *Chem. Eur. J.*, 2005, **11**, 2081–2093and references therein; (*g*) T. Uchimaru, M. Uebayasi, T. Hirose, S. Tsuzuki, A. Yliniemelä, K. Tanabe and K. Taira, *J. Org. Chem.*, 1996, **61**, 1599–1608.

4 (*a*) W. S. Wadsworth, Jr., *Org. React.*, 1977, **25**, 73–253; (*b*) J. I. G. Cadogan, *Organophosphorus Reagents in Organic Synthesis*, Academic Press, New York, 1979; (*c*) B. E. Maryanoff and A. B. Reitz, *Chem. Rev.*, 1989, **89**, 863–927; (*d*) S. E. Kelly, in *Comprehensive Organic Synthesis*, ed. B. M. Trost and I. Fleming, Pergamon Press, Oxford, 1991, vol. 1, pp. 730–817; (*e*) A. W. Johnson, *Ylides and Imines of Phosphorus*, Wiley-Interscience, New York, 1993; (*f*) E. Vedejs and M. J. Peterson, *Top. Stereochem.*, 1994, **21**, 1–157; (*g*) E. Vedejs and M. J. Peterson, *Adv. Carbanion Chem.*, 1996, **2**, 1–85.

5 (*a*) E. L. Muetterties, W. Mahler and R. Schmutzler, *Inorg. Chem.*, 1963, **2**, 613–618; (*b*) E. L. Muetterties, W. Mahler, K. J. Packer and R. Schmutzler, *Inorg. Chem.*, 1964, **3**, 1298–1303; (*c*) G. M. Whiteside and W. M. Bunting, *J. Am. Chem. Soc.*, 1967, **89**, 6801–6802; (*d*) G. M. Whiteside and H. L. Mitchell, *J. Am. Chem. Soc.*, 1969, **91**, 5384–5386.

6 (*a*) J. I. Musher, *Angew. Chem., Int. Ed. Engl.*, 1969, **8**, 54–68; (*b*) W. Kutzelnigg, *Angew. Chem., Int. Ed. Engl.*, 1984, **23**, 272–295.

7 (*a*) M. Nakamoto, S. Kojima, S. Matsukawa, Y. Yamamoto and K.-y. Akiba, *J. Organomet. Chem.*, 2002, **643–644**, 441–452; (*b*) S. Matsukawa, K. Kajiyama, S. Kojima, S.-y. Furuta, Y. Yamamoto and K.-y. Akiba, *Angew. Chem., Int. Ed.*, 2002, **41**, 4718–4722; (*c*) S. Trippett, *Phosphorus Sulfur*, 1976, **1**, 89–98; (*d*) S. Trippett, S., *Pure Appl. Chem.*, 1974, **40**, 595–604; (*e*) G. Buono and J. R. Llinas, *J. Am. Chem. Soc.*, 1981, **103**, 4532–4540; (*f*) M. Eisenhut, H. L. Mitchell, D. D. Traficante, R. J. Kaufman, J. M. Deutch and G. M. Whitesides, *J. Am. Chem. Soc.*, 1974, **96**, 5385–5397; (*g*) C. G. Moreland, G. O. Doak, L. B. Littlefield, N. S. Walker, J. W. Gilje, R. W. Braun and A. H. Cowley, *J. Am. Chem. Soc.*, 1976, **98**, 2161–2165; (*h*) L. V. Griend and R. G. Cavell, *Inorg. Chem.*, 1983, **22**, 1817–1820; (*i*) S. Kumaraswamy, C. Muthiah and K. C. Kumara Swamy, *J. Am. Chem. Soc.*, 2000, **122**, 964–965; (*j*) P. Kommana, S. Kumaraswamy, J. J. Vittal and K. C. Kumara Swamy, *Inorg. Chem.*, 2002, **41**, 2356–2363; (*k*) P. Kommana, N. S. Kumar, J. J. Vittal, E. G. Jayasree, E. D. Jemmis and K. C. Kumara Swamy, *Org. Lett.*, 2004, **6**, 145–148.

8 (*a*) R. Hoffmann, J. M. Howell and E. L. Muetterties, *J. Am. Chem. Soc.*, 1972, **94**, 3047–3058; (*b*) R. S. McDowell and A. Streitwieser, Jr., *J. Am. Chem. Soc.*, 1985, **107**, 5849–5855; (*c*) J. A. Deiters, R. R. Holmes and J. M. Holmes, *J. Am. Chem. Soc.*, 1988, **110**, 7672–7681; (*d*) P. Wang, Y. Zhang, R. Glaser, A. E. Reed, P. v. R. Schleyer and A. Streitwieser, Jr., *J. Am. Chem. Soc.*, 1991, **113**, 55–64; (*e*) H. Wasada and K. Hirao, *J. Am. Chem. Soc.*, 1992, **114**, 16–27; (*f*) G. R. J. Thatcher and A. S. Campbell, *J. Org. Chem.*, 1993, **58**, 2272–2281; (*g*) P. Wang, Y. Zhang, R. Glaser, A. Streitwieser and P. v. R. Schleyer, *J. Comput. Chem.*, 1993, **14**, 522–529; (*h*) B. D. Wladkowski, M. Krauss and W. J. Stevens, *J. Phys. Chem.*, 1995, **99**, 4490–4500.

9 R. S. Berry, *J. Chem. Phys.*, 1960, **32**, 933–938.

10 (*a*) K. Mislow, *Acc. Chem. Res.*, 1970, **3**, 321–331; (*b*) E. L. Muetterties, *Acc. Chem. Res.*, 1970, **3**, 266–273; (*c*) I. Ugi, D. Marquarding, H. Klusacek, P. Gillespie and F. Ramirez, *Acc. Chem. Res.*, 1971, **4**, 288–296; (*d*) P. Gillespie, P. Hoffman, H. Klusacek, D. Marquarding, S. Pfohl, F. Ramirez, E. A. Tsolis and I. Ugi, *Angew. Chem., Int. Ed.*, 1971, **10**, 687–715.

11 J. Moc and K. Morokuma, *J. Am. Chem. Soc.*, 1995, **117**, 11790–11797.

12 J. C. Martin, *Science.*, 1983, **221**, 509–514.

13 (*a*) S. Kojima, K. Kajiyama, M. Nakamoto and K.-y. Akiba, *J. Am. Chem. Soc.*, 1996, **118**, 12866–12867; (*b*) S. Kojima, K. Kajiyama, M. Nakamoto, S. Matsukawa and K.-y. Akiba, *Eur. J. Org. Chem.*, 2006, 218–234.

14 (*a*) Some compounds, which violate the apicophilicity concept, were isolated. In these cases, some sort of steric constraints disallowed the regular configurations: J. Kobayashi, K. Goto and T. Kawashima, *J. Am. Chem. Soc.*, 2001, **123**, 3387–3388; (*b*) J. Kobayashi, K. Goto, T. Kawashima, M. W. Schmidt and S. Nagase, *J. Am. Chem. Soc.*, 2002,

124, 3703–3712; (*c*) S. Vollbrecht, A. Vollbrecht, J. Jeske, P. G. Jones, R. Schmutzler and W.-W. du Mont, *Chem. Ber./Recl*, 1997, **130**, 819–822; (*d*) K. C. Kumara Swamy and N. S. Kumar, *Acc. Chem. Res.*, 2006, **39**, 324–333; (*e*) K. V. P. P. Kumar, N. S. Kumar and K. C. Kumara Swamy, *New J. Chem.*, 2006, **30**, 717–728; (*f*) A. Chandrasekaran, N. V. Timosheva and R. R. Holmes, *Phosphorus, Sulfur, Silicon Relat. Elem.*, 2006, **181**, 1493–1511; (*g*) N. S. Kumar, P. Kommana, J. J. Vittal and K. C. Kumara Swamy, *J. Org. Chem.*, 2002, **67**, 6653–6658.

15 (*a*) X.-D. Jiang, K.-i. Kakuda, S. Matsukawa, H. Yamamichi, S. Kojima and Y. Yamamoto, *Chem. Asian J.*, 2007, **2**, 314–323; (*b*) X.-D. Jiang, S. Matsukawa, H. Yamamichi and Y. Yamamoto, *Heterocycles*, 2007, **73**, 805–824.

16 X.-D. Jiang, S. Matsukawa, H. Yamamichi and Y. Yamamoto, *Inorg. Chem.*, 2007, **46**, 5480–5482.

17 (*a*) K. Kajiyama, M. Yoshimune, M. Nakamoto, S. Matsukawa, S. Kojima and K.-y. Akiba, *Org. Lett.*, 2001, **3**, 1873–1875; (*b*) K. Kajiyama, M. Yoshimune, S. Kojima and K.-y. Akiba, *Eur. J. Org. Chem.*, 2006, 2739–2746.

18 S. Matsukawa, S. Kojima, K. Kajiyama, Y. Yamamoto, K.-y. Akiba, S. Re and S. Nagase, *J. Am. Chem. Soc.*, 2002, **124**, 13154–13170.

19 T. Adachi, S. Matsukawa, M. Nakamoto, K. Kajiyama, S. Kojima, Y. Yamamoto, K.-y. Akiba, S. Re and S. Nagase, *Inorg. Chem.*, 2006, **45**, 7269–7277.

20 C. Reichardt, in *Solvents and Solvent Effects in Organic Chemistry*, Wiley-VCH, Weinheim, 3rd edn, 2003, pp. 472–475.

21 M. Charton, *Prog. Phys. Org. Chem.*, 1981, **13**, 119–251.

22 For the proposed nomenclature system for optically active pentacoordinate molecules, see: J. C. Martin and T. M. Balthazor, *J. Am. Chem. Soc.*, 1977, **99**, 152–162.

23 Z. Otwinowski and W. Minor, *Methods Enzymol.*, 1997, **276**, 307–326.

24 G. M. Sheldrick, *SHELX-97*, University of Göttingen, Göttingen, Germany, 1997.